### ORIGINAL ARTICLE



## Characterization of tumor-associated macrophages in prostate cancer transgenic mouse models

Amber E. de Groot PhD<sup>1,2</sup> | Kayla V. Myers<sup>1,2</sup> | Timothy E. G. Krueger<sup>1,2,3</sup> | Ashley L. Kiemen<sup>4</sup> | Natalia H. Nagy<sup>1</sup> | Alexandria Brame<sup>1</sup> | Vicente E. Torres<sup>1</sup> | Zhongyuan Zhang<sup>1</sup> | Levent Trabzonlu MD<sup>5</sup> | W. Nathaniel Brennen PhD<sup>1,3</sup> | Denis Wirtz PhD<sup>4,6</sup> | Angelo M. De Marzo MD, PhD<sup>1,3,6</sup> | Sarah R. Amend PhD<sup>1,3</sup> | Kenneth J. Pienta MD<sup>1,2,3</sup> |

### Correspondence

Kenneth J. Pienta, MD, Department of Urology, James Buchanan Brady Urological Institute, Johns Hopkins School of Medicine, 600 N. Wolfe Street, Marburg 120, Baltimore, MD 21287, USA.

Email: kpienta1@jhmi.edu

### **Funding information**

Patrick C. Walsh Prostate Cancer Research Fund; National Cancer Institute, Grant/Award Numbers: CA093900, CA143055, CA163124, P50CA58236, U01CA196390, U54CA143803; U.S. Department of Defense, Grant/Award Numbers: W81XWH-17-1-0528, W81XWH-20-1-0353: Prostate Cancer

Foundation

### **Abstract**

Background: Tumor-associated macrophages (TAMs) are critical components of the tumor microenvironment (TME) in prostate cancer. Commonly used orthotopic models do not accurately reflect the complete TME of a human patient or the natural initiation and progression of a tumor. Therefore, genetically engineered mouse models are essential for studying the TME as well as advancing TAM-targeted therapies. Two common transgenic (TG) models of prostate cancer are Hi-Myc and transgenic adenocarcinoma of the mouse prostate (TRAMP), but the TME and TAM characteristics of these models have not been well characterized. Methods: To advance the Hi-Myc and TRAMP models as tools for TAM studies.

macrophage infiltration and characteristics were assessed using histopathologic, flow cytometric, and expression analyses in these models at various timepoints during tumor development and progression.

Results: In both Hi-Myc and TRAMP models, macrophages adopt a more pro-tumor phenotype in higher histological grade tumors and in older prostate tissue. However, the Hi-Myc and TRAMP prostates differ in their macrophage density, with Hi-Myc tumors exhibiting increased macrophage density and TRAMP tumors exhibiting decreased macrophage density compared to age-matched wild type mice. Conclusions: The macrophage density and the adenocarcinoma cancer subtype of Hi-Myc appear to better mirror patient tumors, suggesting that the Hi-Myc model is the more appropriate in vivo TG model for studying TAMs and TME-targeted therapies.

### KEYWORDS

Hi-Myc, pro-tumor, TAM, TRAMP, tumor microenvironment

This is an open access article under the terms of the Creative Commons Attribution-NonCommercial License, which permits use, distribution and reproduction in any medium, provided the original work is properly cited and is not used for commercial purposes.

© 2021 The Authors. *The Prostate* published by Wiley Periodicals LLC

The Prostate. 2021;1–19. wileyonlinelibrary.com/journal/pros

<sup>&</sup>lt;sup>1</sup>Department of Urology, James Buchanan Brady Urological Institute, Johns Hopkins School of Medicine, Baltimore, Maryland, USA

<sup>&</sup>lt;sup>2</sup>Department of Pharmacology and Molecular Sciences, Johns Hopkins School of Medicine, Baltimore, Maryland, USA

<sup>&</sup>lt;sup>3</sup>Department of Oncology, Johns Hopkins School of Medicine, Baltimore, Maryland, USA

<sup>&</sup>lt;sup>4</sup>Department of Chemical and Biomolecular Engineering, Johns Hopkins Whiting School of Engineering, Baltimore, Maryland, USA

<sup>&</sup>lt;sup>5</sup>Department of Pathology and Laboratory Medicine, Loyola University Medical Center, Maywood, Illinois, USA

<sup>&</sup>lt;sup>6</sup>Department of Pathology, Johns Hopkins School of Medicine, Baltimore, Maryland, USA

### 1 | INTRODUCTION

Prostate cancer tumor growth and disease progression are highly influenced by noncancerous host cells within the tumor microenvironment (TME). One particularly important TME cell type in prostate cancer is the tumor-associated macrophage (TAM) which can comprise up to 50% of prostate cancer bone metastases. Examination of prostate cancer patient tissues revealed that the extent of infiltration of tumor tissue by TAMs was increased in aggressive and advanced disease. In addition, TAMs in prostate cancer as well as other cancers are known to contribute to tumorigenesis.

Macrophages are a plastic cell type and adopt different functions in response to signaling molecules in their environment. There are an array of subtypes that a macrophage can adopt which are categorized by the polarization stimuli, gene expression, and functional readouts (i.e., cytokine secretion, phagocytosis, and T cell activation).  $^{4-6}$  Given the plasticity of macrophages and their ability to repolarize, macrophages often do not fit neatly into these subtypes making classification of TAMs based on canonical subtypes complicated and imperfect.  $^{4.5.7-10}$ 

To date, the field has relied on an M1–M2 dichotomy spectrum to associate macrophage characteristics with either antitumor (M1) or pro-tumor (M2) functions. While this has proved useful in providing a common language with which to describe TAMs, the field has advanced in its understanding of the nuances of TAM gene expression and behavior. It is becoming increasingly clear that the M1–M2 model no longer suffices in encapsulating the complexity and key characteristics of TAMs. In light of this, we consider the terms "M2-like" and "pro-tumor" to be appropriate means for referring to such TAMs that share tissue remodeling and immunesuppressing characteristics with M2s but differ in expression of specific characteristic genes.

The majority of TAMs associated with prostate cancer lesions are pro-tumor and M2-like. Similar to M2s, these TAMs promote tissue remodeling, cell growth and proliferation, and suppress a CD8<sup>+</sup> cytotoxic T cell response which altogether support tumors.<sup>7,13</sup> Given their pro-tumor functions and their prevalence in prostate cancer, targeting pro-tumor M2-like TAMs provides a pressing and promising adjunct therapeutic strategy.

To study effective ways to target M2-like TAMs in patients, it is important to have accurate in vivo prostate cancer models. Of the available prostate cancer mouse models, transgenic (TG) mice are among the most accurate in vivo models of tumor initiation and the evolving TME. Other models such as xenograft or syngeneic injected cancer cell lines and allograft tumor transplantation are insufficient given their methods of tumor induction. Such injected tumor models are poor models for tumor initiation as they involve implantation of bulk tumors that lack any semblance of the original tissue architecture seen in early-stage tumors and native TME components and heterogeneity. Additionally, because of the way these tumors are initiated, these models rely heavily on infiltrating host cells to reconstitute the TME which may not accurately reflect that of a patient's tumor. However, in TG mouse models, tumors are initiated

using the host's cells which shapes the tissue in a manner that is more histologically consistent with early-stage patient tumors. This provides a more accurate model for studying both tumor initiation and the TME.

Two common prostate cancer TG mouse models are the Hi-Myc and transgenic adenocarcinoma of the mouse prostate (TRAMP) models. The Hi-Myc model is genetically engineered to express the human c-myc oncogene under the prostate-specific probasin promoter and two androgen-regulated regions. 16 Hi-Myc mice develop prostatic intraepithelial neoplasia (PIN) as early as 2 weeks and adenocarcinoma tumors are observed in all mice by 6 months. The TRAMP model contains a rat probasin promoter-driven simian virus 40 large tumor T antigen (SV40 T-Ag) gene which when expressed acts as an oncoprotein by inhibiting Rb and p53 tumor suppressors. 17 While the line was initially thought to model adenocarcinoma, the large invasive tumors that develop in TRAMP mice were later found to be best classified as neuroendocrine prostate cancer. 18 Carcinogenic tissue from these mice is observed in all mice by 10-12 weeks. 18,19 These models offer a means for studying the TME and tumor initiation that more closely resembles patient tumor development.

These two TG models have been widely used and are advantageous for prostate cancer studies. The histology and characteristics of the carcinogenic cells in these models are well characterized and cell lines developed from these models have proven to be useful tools. 20,21 However, with increased interest in immunotherapeutic treatments for prostate cancer, it has become increasingly clear how important it is to understand the immune components of these models to inform development of immune-related prostate cancer therapeutics. Our work endeavors to describe the macrophage characteristics and infiltration in Hi-Myc and TRAMP prostates over time and with tumor growth in these models.

### 2 | MATERIALS AND METHODS

### 2.1 | Mouse models

The Johns Hopkins Institutional Animal Care and Use Committee approved all experiments involving mice (protocol # MO19M41). FVB/N Hi-Myc and FVB/N TRAMP mice were a gift from Brian Simons (Baylor University). Mice were bred in monogamous pairs with a transgene heterozygote female and a nontransgene bearing male. Mice containing the transgene were identified by tail snip DNA extraction with Hot Shot Lysis Buffer (25 mM NaOH, 0.2 mM ethylenediaminetetraacetic acid [EDTA]) and PCR with *Taq* DNA polymerase (100021276; NEB) using primers forward 5′-AAACAT GATGACTACCAAGCTTGGC-3′ and reverse 5′-ATGATAGCATC TTGTTCTTAGTCTTTTTCTTAATAGGG-3′ for Hi-Myc and forward 5′-GCGCTGCTGACTTTCTAAACATAAG-3′ and reverse 5′-GAGCTC ACGTTAAGTTTTGATGTGT-3′ for TRAMP. Mice were euthanized using CO<sub>2</sub> asphyxiation. Prostates were micro-dissected using protocols described previously.<sup>22</sup>

**TABLE 1** Upregulated differentially expressed genes (DEGs) in Hi-Myc 2-month transgenic (TG) compared to wild type (WT) prostate macrophages

			Normalize	
Gene	Accession #	Fold change	WT	TG
Rnase2a <sup>a</sup>	NM_053113.2	9.05	32.42	293.26
Adam8 <sup>a</sup>	NM_007403.2	3.06	89.44	273.26
Tgm2 <sup>a</sup>	NM_009373.3	2.95	220.23	648.72
Clec7a <sup>a</sup>	NM_020008.2	2.51	320.85	805.34
Fyn <sup>a</sup>	NM_008054.2	2.13	77.14	164.40
Retnla <sup>a</sup>	NM_020509.3	1.98	2343.21	4642.10
Isg15 <sup>a,b</sup>	NM_015783.3	1.78	270.54	480.98
C4a <sup>a</sup>	NM_011413.2	1.72	139.74	241.05
Trem2 <sup>a</sup>	NM_031254.2	1.67	181.11	302.14
Fcgr1 <sup>a</sup>	NM_010186.5	1.63	183.34	298.81
Ctsd <sup>a,b</sup>	NM_009983.2	1.60	2082.73	3329.11
Fcgr2b <sup>a,b</sup>	NM_001077189.1	1.59	657.35	1043.06
Osm <sup>a</sup>	NM_001013365.2	1.54	690.89	1065.27
Psmb8 <sup>a</sup>	NM_010724.2	1.53	226.94	347.69
Apoe <sup>a,b</sup>	NM_001305844.1	1.52	7775.29	11849.07
Csf2rb <sup>a</sup>	NM_007780.4	1.51	503.07	759.80
II1rn <sup>a</sup>	NM_031167.5	1.50	2134.15	3191.37
Grn <sup>a,b</sup>	NM_008175.4	1.42	453.88	643.16

Abbreviation: TRAMP, transgenic adenocarcinoma of the mouse prostate. <sup>a</sup>Commonly upregulated across cohorts in TG compared to strainmatched, age-matched WT.

### 2.2 | Tissue fixation and immunohistochemistry

For prostates that were fixed, tissue was incubated in 10% neutral buffered saline for 48 h and stored in 70% ethanol. Tissue was paraffin-embedded, sectioned, and stained with hematoxylin and eosin by the Johns Hopkins Oncology Tissue Services Core. Immunolabeling for F4/80 was performed by the Johns Hopkins Oncology Tissue Services Core on formalin-fixed, paraffin embedded sections. Briefly, following dewaxing and rehydration, slides were immersed in 1% Tween-20, then heat-induced antigen retrieval was performed in a steamer using Target Retrieval Solution (S170084-2; Dako) for 45 min. Slides were rinsed in PBST and endogenous peroxidase and phosphatase was blocked (S2003; Dako) and sections were then incubated with primary antibody; anti-F4/80 (1:2000 dilution; MCA497R, lot 1365, Serotec; Bio-Rad) for 45 min at room temperature, followed by incubation with rabbit anti-rat antibody (1:500 dilution, Al-4001, lot ZC0603; Vectorlab). The linking antibodies were detected by 30-min incubation with HRP-labeled antirabbit secondary antibody (PV6119; Leica Microsystems) followed

**TABLE 2** Downregulated differentially expressed genes (DEGs) in Hi-Myc 2-month transgenic (TG) compared to wild type (WT) prostate macrophages

prostate m	acrophages		Mauri Pe	Lanumer
Gene	Accession #	Fold change	Normalized WT	TG
ld1	NM_010495.2	-3.07	133.04	43.32
Hpgd <sup>a</sup>	NM_008278.2	-2.99	397.99	133.30
Mmp13	NM_008607.1	-2.79	741.20	265.48
II12b <sup>a</sup>	NM_001303244.1	-2.65	10624.92	4003.38
Hpgds	NM_019455.4	-2.59	618.22	238.83
Ceacam1	NM_001039185.1	-2.57	279.49	108.86
Cxcl13 <sup>a</sup>	NM_018866.2	-2.39	169.93	71.09
Cyr61	NM_010516.1	-2.17	181.11	83.31
Birc2	NM_007465.2	-2.12	276.13	129.97
Cdh1	NM_009864.2	-2.07	206.82	99.97
Tlr1	NM_030682.1	-1.99	404.69	203.28
Mmp12 <sup>a</sup>	NM_008605.3	-1.98	4029.06	2038.35
Stat5a	NM_011488.2	-1.96	211.29	107.75
Mmp9 <sup>a</sup>	NM_013599.2	-1.89	305.20	161.07
Tuba4a <sup>a</sup>	NM_009447.3	-1.87	242.59	129.97
Hivep1	NM_007772.2	-1.83	302.96	165.51
Cd163 <sup>a</sup>	NM_053094.2	-1.75	382.34	218.83
Ripk2	NM_138952.3	-1.75	338.74	193.28
Cd180	NM_008533.2	-1.69	238.12	141.07
Fosb	NM_008036.2	-1.68	493.01	293.26
Rin2	NM_028724.4	-1.67	251.54	151.07
Rgs1	NM_015811.1	-1.67	2526.55	1508.49
Cxcl1	NM_008176.1	-1.67	11723.85	7040.35
lgf1r	NM_010513.2	-1.65	256.01	155.51
Cd86	NM_019388.3	-1.61	2294.02	1427.40
Adamts1 <sup>a</sup>	NM_009621.4	-1.59	323.09	203.28
Klf4	NM_010637.3	-1.59	402.46	253.27
II1b	NM_008361.3	-1.58	7821.12	4949.79
Malt1	NM_172833.2	-1.56	906.65	582.07
Ccl22	NM_009137.2	-1.55	1119.06	720.92
Cybb	NM_007807.2	-1.55	1771.94	1144.14
II1a	NM_010554.4	-1.54	880.94	572.07
Cxcl2	NM_009140.2	-1.53	12730.00	8321.12
Nfkbiz <sup>a</sup>	NM_030612.1	-1.50	2095.02	1394.07
Clic4	NM_013885.2	-1.48	745.67	505.42
Icosl <sup>a</sup>	NM_015790.3	-1.47	1548.35	1051.94
Ccr7	NM_007719.2	-1.46	960.31	656.49

(Continues)

 $<sup>^{\</sup>rm b}\text{Commonly}$  upregulated across cohorts in Hi-Myc 2 months, Hi-Myc 6 months, TRAMP 2 months, and TRAMP 5 months.

TABLE 2 (Continued)

Gene	Accession #	Fold change	Normalized WT	d counts TG
Icam1	NM_010493.2	-1.45	700.95	482.09
Msr1	NM_001113326.1	-1.44	1482.39	1028.61
Dusp2	NM_010090.2	-1.44	765.79	530.97
Gem <sup>a</sup>	NM_010276.3	-1.43	851.87	594.29
Nfkb1	NM_008689.2	-1.43	1632.19	1144.14
Nr4a1 <sup>a</sup>	NM_010444.1	-1.42	822.81	578.73
Irf1 <sup>a</sup>	NM_008390.1	-1.42	1181.66	834.22
Ptprc	NM_011210.3	-1.42	673.00	474.32
Skil	NM_011386.2	-1.40	1942.98	1384.08
Ptgs2	NM_011198.3	-1.39	6118.50	4402.16
Birc3	NM_007464.3	-1.39	746.79	538.75
NIrp3	NM_145827.3	-1.38	1617.66	1171.91
Tgfbr2	NM_029575.3	-1.37	1953.04	1428.51
Ccl3 <sup>a</sup>	NM_011337.1	-1.36	18022.34	13210.92
Jun <sup>a</sup>	NM_010591.2	-1.36	2035.77	1496.27
Cd83	NM_009856.2	-1.26	10641.69	8422.20

<sup>&</sup>lt;sup>a</sup>Commonly downregulated across cohorts in TG compared to strainmatched, age-matched WT.

by detection with 3,3'-diaminobenzidine (D4293; Sigma-Aldrich), counterstaining with Mayer's hematoxylin, dehydration, and mounting.

### 2.3 | Immunohistochemistry (IHC) quantification

F4/80 IHC sections were scanned at ×20 resolution. Regions of PIN, cribriform PIN/carcinoma in situ (CribPIN/CIS), invasive adenocarcinoma, or higher-grade carcinoma were identified by a pathologist. QuPath version 0.1.2 was used to define analysis regions and quantify DAB staining as a function of number of brown DAB pixels over total number of stained (DAB or hematoxylin) pixels in the defined region. One 6-month Hi-Myc wild type (WT) mouse, one 6-month Hi-Myc TG mouse, one 2-month TRAMP TG mouse, and one 5-month TRAMP WT mouse were identified as statistical outliers and removed from all IHC analyses.

### 2.4 | Flow-cytometric macrophage analysis

Prostate tissue was subjected to single cell dissociation using the MACS Mouse Tumor Dissociation Kit protocol and gentleMACS Dissociator (Miltenyi). Suspended cells were blocked with rat serum (012-000-120;

**TABLE 3** Upregulated differentially expressed genes (DEGs) in Hi-Myc 6-month transgenic (TG) compared to wild type (WT) prostate macrophages

prostate ma		Fold	Normalized	counts
Gene	Accession #	change	WT	TG
Arg1 <sup>b</sup>	NM_007482.3	At least 31.39	Below thres- hold	627.79
Rnase2a <sup>a</sup>	NM_053113.2	At least 10.14	Below thres- hold	202.72
Emp1 <sup>b</sup>	NM_010128.4	9.12	36.21	330.38
Adam8 <sup>a,b</sup>	NM_007403.2	7.93	32.11	254.62
Tgm2 <sup>a,b</sup>	NM_009373.3	7.24	142.80	1033.93
II1rn <sup>a</sup>	NM_031167.5	6.27	366.22	2294.43
Vegfa <sup>b</sup>	NM_001025250.3	6.23	122.30	761.77
Cd274	NM_021893.2	5.52	120.25	664.27
Cxcl3	NM_203320.2	4.83	57.39	277.07
Ccl8 <sup>b</sup>	NM_021443.2	4.45	178.33	793.33
Csf2rb <sup>a,b</sup>	NM_007780.4	3.69	203.61	751.95
Irf7 <sup>b</sup>	NM_016850.2	3.67	38.26	140.29
Clec7a <sup>a</sup>	NM_020008.2	3.57	493.98	1762.73
Arg2	NM_009705.2	3.56	34.85	124.16
Nfil3	NM_017373.3	3.33	198.14	659.36
Cc17	NM_013654.3	3.28	364.17	1195.26
Fn1 <sup>b</sup>	NM_010233.1	3.23	126.40	408.24
Ccr1 <sup>b</sup>	NM_009912.4	3.16	142.11	448.92
Ctsd <sup>a,b,c</sup>	NM_009983.2	3.14	2308.67	7239.61
Cd84 <sup>b</sup>	NM_001252472.1	3.11	168.08	523.28
Fcgr2b <sup>a,b,c</sup>	NM_001077189.1	3.10	566.41	1757.82
Cytip	NM_139200.4	2.97	179.69	533.10
Osm <sup>a</sup>	NM_001013365.2	2.93	539.08	1577.55
Trem1	NM_021406.5	At least 2.91	Below thres- hold	58.22
Furin	NM_011046.2	2.64	380.57	1003.07
Stat1	NM_009283.3	2.55	73.79	187.99
Cxcl9	NM_008599.2	2.53	38.26	96.80
Hif1a	NM_010431.2	2.49	331.37	824.20
Anxa1 <sup>b</sup>	NM_010730.2	2.40	59.44	142.39
Cd80	NM_009855.2	2.35	64.22	150.81
Fcgr4 <sup>b</sup>	NM_144559.1	2.33	127.77	298.11
Nampt	NM_021524.1	2.33	392.18	911.88
Isg15 <sup>a,b,c</sup>	NM_015783.3	2.28	164.66	375.27

TABLE 3 (Continued)

		Fold	Normalized	
Gene	Accession #	change	WT	TG
Crem	NM_001110853.1	2.18	53.98	117.84
Ccr2 <sup>b</sup>	NM_009915.2	2.17	76.52	166.24
II10	NM_010548.1	2.12	64.91	137.48
Fyn <sup>a,b</sup>	NM_008054.2	2.11	57.39	121.35
Grn <sup>a,b,c</sup>	NM_008175.4	2.04	426.34	867.69
Cxcr4	NM_009911.3	2.03	251.43	509.95
Ccl2	NM_011333.3	2.03	1663.01	3380.96
Siglec1	NM_011426.3	2.00	56.71	113.63
Ccl6 <sup>b</sup>	NM_009139.2	1.99	116.15	230.78
C4a <sup>a,b</sup>	NM_011413.2	1.97	174.23	343.71
Tlr8 <sup>b</sup>	NM_133212.2	1.94	168.76	326.87
S100a11	NM_016740.3	1.92	144.85	277.77
Tnfrsf1b	NM_011610.3	1.89	190.62	360.54
H2-D1	NM_010380.3	1.86	2771.23	5157.72
Pdgfa	NM_008808.3	1.86	237.08	440.51
Txn1 <sup>b</sup>	NM_011660.3	1.86	506.97	942.04
Anxa4	NM_013471.2	1.82	215.22	391.41
Alcam	NM_009655.1	1.81	94.29	170.45
Retnla <sup>a</sup>	NM_020509.3	1.80	1408.16	2532.21
Ccl9 <sup>a</sup>	NM_011338.2	1.80	871.82	1569.83
Fem1c	NM_173423.4	1.80	325.22	584.30
Apoe <sup>a,b,c</sup>	NM_001305844.1	1.79	13407.25	24039.21
Ptgs2	NM_011198.3	1.76	1920.59	3371.14
Ccr5	NM_009917.5	1.72	349.82	601.14
II2rg	NM_013563.3	1.71	79.94	136.78
Msr1	NM_001113326.1	1.69	537.71	906.27
Ccl5	NM_013653.1	1.67	182.43	305.13
Trem2 <sup>a,b</sup>	NM_031254.2	1.62	342.30	553.44
Psmb8 <sup>a</sup>	NM_010724.2	1.61	284.91	458.74
Cebpb	NM_009883.3	1.61	1694.44	2727.22
Ctss	NM_021281.2	1.61	4061.87	6543.07
Cd47 <sup>b</sup>	NM_010581.3	1.57	217.95	342.30
Fcgr1 <sup>a,b</sup>	NM_010186.5	1.56	377.83	588.51
Serpine1	NM_008871.2	1.56	233.67	364.75
Smad7	NM_001042660.1	1.56	183.79	286.89
Plaur	NM_011113.3	1.55	262.36	406.14
II17ra	NM_008359.1	1.55	181.06	280.58
	-			

TABLE 3 (Continued)

Gene	Accession #	Fold change	Normalized WT	counts
Mif <sup>b</sup>	NM_010798.2	1.51	148.26	223.76
H2-Q1	NM_010390.3	1.50	663.43	994.65
Ctnnb1 <sup>b</sup>	NM_007614.2	1.47	525.41	771.59
C1qb <sup>b</sup>	NM_009777.2	1.46	3249.50	4741.06
Malt1	NM_172833.2	1.43	283.55	406.84
Syk	NM_001198977.1	1.43	315.66	451.73
Cstb	NM_007793.3	1.43	1421.83	2036.99
ler3	NM_133662.2	1.42	924.43	1313.81
Rhog	NM_019566.3	1.42	610.13	866.99
Lipa	NM_021460.3	1.40	513.80	716.88
ltgb1	NM_010578.1	1.39	680.51	946.25
II1a	NM_010554.4	1.38	474.85	654.45
Cdkn1a	NM_007669.4	1.38	512.43	707.76
Psme2	NM_001029855.1	1.37	392.18	537.31
Cd14	NM_009841.3	1.32	2825.20	3740.10
ld2	NM_010496.3	1.29	4426.04	5713.27

Abbreviation: TRAMP, transgenic adenocarcinoma of the mouse prostate. <sup>a</sup>Commonly upregulated across cohorts in TG compared to strainmatched, age-matched WT.

 $^{\rm b}\text{Commonly}$  upregulated across cohorts in Hi-Myc 6 months and TRAMP 5 months.

<sup>c</sup>Commonly upregulated across cohorts in Hi-Myc 2 months, Hi-Myc 6 months, TRAMP 2 months, and TRAMP 5 months.

Jackson ImmunoResearch), stained with FVS570 viability dye (1 µl/ml, 564995; BD Biosciences) in the dark for 15 min at room temperature. Samples were washed with phosphate-buffered saline (PBS) and incubated with Myeloid extracellular antibody panel (Table S1) or corresponding isotype panels diluted in Brilliant Stain Buffer (566349; BD Biosciences) in the dark for 30 min at 4°C. Cells were washed with FACS buffer (1X PBS, 1% bovine serum albumin, 2 mM EDTA), fixed with 1X Fixation Buffer (420801; BioLegend) in the dark for 20 min at room temperature, and stored overnight in FACS buffer at 4°C. Samples were incubated in 1X FoxP3 Fix/Perm Solution (421401; BioLegend) in the dark for 20 min at room temperature and washed with 1X FoxP3 Perm Buffer (421402; BioLegend). Cells were resuspended with Myeloid intracellular antibody panel (Table S1) or corresponding isotype panels diluted in FACS buffer in the dark for 30 min at room temperature under gentle agitation. Cell suspensions were washed with FACS buffer and analyzed with a Gallios flow cytometer (Beckman Coulter Life Sciences). Macrophages were defined as FVS570<sup>-</sup>CD45<sup>+</sup>CD11b<sup>+</sup>F4/80<sup>+</sup>CD68<sup>+</sup> cells.

(Continues)

**TABLE 4** Downregulated differentially expressed genes (DEGs) in Hi-Myc 6-month transgenic (TG) compared to wild type (WT) prostate macrophages

prostate ma			Normalized	
Gene	Accession #	Fold change	WT	TG
Adamts1 <sup>a,b</sup>	NM_009621.4	-6.18	663.43	107.32
Fscn1 <sup>b</sup>	NM_007984.2	-4.38	116.83	26.65
Mmp9 <sup>a,b</sup>	NM_013599.2	-4.21	333.42	79.26
Hpgd <sup>a,b</sup>	NM_008278.2	-3.62	556.16	153.62
Cd163 <sup>a,b</sup>	NM_053094.2	-3.50	334.11	95.40
Cxcl13 <sup>a,b</sup>	NM_018866.2	-2.69	215.22	79.96
Btg2 <sup>b</sup>	NM_007570.2	-2.42	1991.65	823.50
Pf4	NM_019932.4	-2.26	481.69	213.24
Alox5	NM_009662.2	-2.24	217.95	97.50
Jun <sup>a,b</sup>	NM_010591.2	-2.19	4083.73	1863.74
Mmp12 <sup>a,b</sup>	NM_008605.3	-2.15	3037.69	1410.60
Tuba4a <sup>a,b</sup>	NM_009447.3	-2.11	182.43	86.28
H2-Ob <sup>b</sup>	NM_010389.3	-2.01	191.99	95.40
Icosl <sup>a,b</sup>	NM_015790.3	-1.94	950.39	491.01
Gem <sup>a,b</sup>	NM_010276.3	-1.88	465.29	247.61
Nfkbiz <sup>a,b</sup>	NM_030612.1	-1.74	1987.55	1145.46
H2-Eb1 <sup>b</sup>	NM_010382.2	-1.73	204.97	118.54
Tnf <sup>b</sup>	NM_013693.2	-1.72	1598.10	929.41
Smad1	NM_008539.3	-1.69	136.65	80.67
Gas6	NM_019521.2	-1.65	760.45	461.55
Irf1 <sup>a,b</sup>	NM_008390.1	-1.64	698.96	427.18
Klf10 <sup>b</sup>	NM_013692.2	-1.63	230.25	141.69
II12b <sup>a,b</sup>	NM_001303244.1	-1.62	1506.55	928.71
Stab1	NM_138672.2	-1.60	758.40	472.77
Col14a1 <sup>b</sup>	NM_181277.3	-1.56	642.93	411.05
Myc <sup>b</sup>	NM_010849.4	-1.55	194.04	125.56
F11r <sup>b</sup>	NM_172647.2	-1.48	243.23	164.14
Insig1 <sup>b</sup>	NM_153526.5	-1.47	502.18	340.90
Marcksl1 <sup>b</sup>	NM_010807.4	-1.45	611.50	422.27
Ccl3 <sup>a,b</sup>	NM_011337.1	-1.44	14366.52	10008.21
Nr4a1 <sup>a,b</sup>	NM_010444.1	-1.43	854.73	598.33
Ccl4 <sup>b</sup>	NM_013652.1	-1.43	3440.12	2404.55
H2-Ea-ps <sup>b</sup>	NM_010381.2	-1.35	4549.02	3365.53
Plau <sup>b</sup>	NM_008873.2	-1.35	2649.61	1958.43
Atf3 <sup>b</sup>	NM_007498.3	-1.33	6386.94	4802.09

Abbreviation: TRAMP, transgenic adenocarcinoma of the mouse prostate. <sup>a</sup>Commonly downregulated across cohorts in TG compared to strain-matched, age-matched WT.

 $^{\rm b}\text{Commonly}$  downregulated across cohorts in Hi-Myc 6 months and TRAMP 5 months.

### 2.5 | Three-dimensional (3D) cell density analysis

Formalin-fixed paraffin-embedded prostate of a representative 14-month-old TG Hi-Myc mouse was serially sectioned into 150 4-  $\mu$ m layers and stained in the following pattern: hematoxylin and eosin (H&E), F4/80 IHC, skip, H&E, F4/80, skip, and so on. H&E and F4/80 stains were scanned at  $\times 20$  resolution. H&E stains were used to calculate total cell density of nucleated cells. The individual tissue images were aligned into a digital tissue volume using a nonlinear image registration program executed in MATLAB 2020a. Overall cell counts were determined using the hematoxylin channel of the images, and macrophage cell counts were determined using the antibody channel of the F4/80 stained IHC sections. Correction factors were used to estimate the true 3D cell count from the serial 2D images. 3D cell density as a function of distance from regions of interest were calculated for a number of locations in the tissue. Regions of carcinogenic tissue were identified by a pathologist.

### 2.6 | Macrophage gene expression

Prostate tissue was subjected to single cell dissociation using enzymatic digestion. Tissue was incubated in a collagenase and hyaluronidase mixture (07912; STEMCELL Technologies) in DMEM/F12K media supplemented with 5% heat-inactivated fetal bovine serum (FBS) for 3 h at 37°C under agitation. Red blood cell lysis was performed with a 1:4 mixture of Hank's Balanced Salt Solution Modified supplemented with 2% heat inactivated FBS and 1% wt/vol ammonium chloride in HBSS. Tissue was further digested using a 5:1 mixture of 5 U/ml Dispase (07913: STEMCELL Technologies) and 1 mg/ml DNase I (07469; STEM-CELL Technologies) with continuous mild agitation for 1 min before filtering through a 40-µm cell strainer. Due to the low cell and macrophage numbers, equivalent cell numbers from each of 10 mice within a cohort were pooled following single cell dissociation. Suspended cells were washed (PBS, 0.5% bovine serum albumin, 2 mM EDTA), blocked with mouse Fc block (Rat antimouse CD16/CD32, clone 2.4G2, 553141; BD Biosciences), and incubated with APC-conjugated anti-mouse CD11b (101212; Biolegend) and PE-conjugated anti-mouse F4/80 (123110; Biolegend) in the dark for 45 min at 4°C. Cells were washed and incubated with 1 µg/million cells 7-aminoactinomycin D (7AAD, A1310; Thermo Fisher Scientific) for 10 min before sorting up to 20 million CD11b<sup>+</sup>F4/80<sup>+</sup>7AAD<sup>-</sup> cells into Qiazol lysis buffer (Qiagen) using a FACSAria II cell sorter (BD Biosciences). RNA was purified using the miRNeasy Micro Kit (Qiagen). Expression levels of 770 immune-related genes were assessed by mouse nCounter Myeloid Innate Immunity Panel and custom Panel Plus (NanoString Technologies) containing the following RNA transcripts listed in Table S2. Hybridization for each sample was performed using 20 ng of RNA measured by Bioanalyzer

**TABLE 5** Upregulated differentially expressed genes (DEGs) in TRAMP 2-month transgenic (TG) compared to wild type (WT) prostate macrophages

Gene	Accession #	Fold change	Normalized WT	counts
Cd84 <sup>a</sup>	NM_001252472.1	4.83	53.8	260.11
Tspan8	NM_001168680.1	4.83	89.1	430.58
Lpl	NM_008509.2	4.21	53.8	226.31
II1a	NM_010554.4	3.43	312.7	1071.3
Clec7a	NM_020008.2	3.22	154.67	498.18
Retnla	NM_020509.3	3.00	1220.54	3666.53
Ptprc	NM_011210.3	2.90	248.82	721.55
Arg2	NM_009705.2	2.82	67.25	189.57
Crem	NM_001110853.1	2.81	79.02	221.9
II13ra1	NM_133990.4	2.44	164.76	401.19
Gpr65	NM_008152.2	2.33	147.94	345.34
Msr1	NM_001113326.1	2.32	593.46	1374.03
Itgav	NM_008402.2	2.29	206.79	473.2
Ctss	NM_021281.2	2.25	2311.63	5197.81
Rgs1	NM_015811.1	2.21	995.26	2201.39
Cd36	NM_007643.3	2.21	479.14	1061.02
Nampt	NM_021524.1	2.19	433.75	947.86
Isg15 <sup>a,b</sup>	NM_015783.3	2.15	257.22	554.02
Hpgds	NM_019455.4	2.14	210.15	449.68
Ell2	NM_138953.2	2.13	122.73	261.58
Skil	NM_011386.2	2.12	1055.79	2239.6
Tnfaip8	NM_134131.2	2.10	215.19	451.15
Malt1	NM_172833.2	1.99	450.56	897.9
Anxa4	NM_013471.2	1.98	257.22	509.93
Tgfbr1	NM_009370.2	1.94	1289.47	2498.24
Hif1a	NM_010431.2	1.93	376.59	727.43
Fcgr2b <sup>a,b</sup>	NM_001077189.1	1.91	401.8	767.11
H2-D1	NM_010380.3	1.89	2686.54	5090.53
Txn1 <sup>a</sup>	NM_011660.3	1.86	536.3	996.36
Ccl2	NM_011333.3	1.86	3927.25	7286.04
Grn <sup>a,b</sup>	NM_008175.4	1.84	430.38	793.56
Ptgs2	NM_011198.3	1.84	4171.02	7688.7
ltgb1	NM_010578.1	1.84	633.81	1163.89
Mrc1	NM_008625.1	1.83	911.2	1669.41
Fem1c	NM_173423.4	1.82	482.5	880.26
Ctsd <sup>a,b</sup>	NM_009983.2	1.81	3263.18	5895.85
S100a11	NM_016740.3	1.79	198.38	355.63

TABLE 5 (Continued)

IADLL	(Continuca)			
Gene	Accession #	Fold change	Normalized WT	TG
Cxcl10	NM_021274.1	1.77	2123.34	3763.52
Ccr1 <sup>a</sup>	NM_009912.4	1.76	161.39	283.62
Ceacam1	NM_001039185.1	1.74	193.34	336.53
Apoe <sup>a,b</sup>	NM_001305844.1	1.73	10460.34	18115.18
Cd86	NM_019388.3	1.73	1284.43	2219.02
Ccl12	NM_011331.2	1.72	1202.05	2064.72
lfnb1	NM_010510.1	1.71	769.98	1316.72
Birc3	NM_007464.3	1.69	440.47	743.59
Ccl3	NM_011337.1	1.64	12191.97	19981.51
Gnai3	NM_010306.2	1.62	258.9	418.82
Cd274	NM_021893.2	1.60	482.5	772.98
Vegfa <sup>a</sup>	NM_001025250.3	1.55	285.8	442.34
Ccl7	NM_013654.3	1.55	1269.3	1972.14
Cybb	NM_007807.2	1.51	1101.18	1666.47
Peli1	NM_023324.2	1.48	521.17	770.05
II17ra	NM_008359.1	1.48	479.14	709.79
Mafb	NM_010658.2	1.47	909.52	1337.29
Osm	NM_001013365.2	1.42	793.52	1127.15
Cxcr4	NM_009911.3	1.42	585.05	830.3
Cdc42	NM_009861.1	1.38	3024.46	4185.29
II1rn	NM_031167.5	1.34	2928.63	3938.4

Abbreviation: TRAMP, transgenic adenocarcinoma of the mouse prostate. <sup>a</sup>Commonly upregulated across cohorts in TG compared to strainmatched, age-matched WT.

<sup>b</sup>Commonly upregulated across cohorts in Hi-Myc 2 months, Hi-Myc 6 months, TRAMP 2 months, and TRAMP 5 months.

**TABLE 6** Downregulated differentially expressed genes (DEGs) in TRAMP 2-month transgenic (TG) compared to wild type (WT) prostate macrophages

Gene	Accession #	Fold change	Normalize WT	d counts TG
Gsn <sup>a</sup>	NM_146120.3	-1.72	692.65	402.66
Pf4	NM_019932.4	-1.70	630.45	370.33
Cxcl3 <sup>a</sup>	NM_203320.2	-1.69	659.03	389.43
Marcksl1 <sup>a</sup>	NM_010807.4	-1.56	1696.32	1086
Hist2h2aa1	NM_013549.2	-1.46	801.93	548.14
Vasp <sup>a</sup>	NM_009499.2	-1.44	1299.56	905.24
Sqstm1 <sup>a</sup>	NM_011018.2	-1.36	7950.33	5859.11

 $^{\rm a}\text{Commonly}$  downregulated across cohorts in TG compared to strainmatched, age-matched WT.

(Continues)

TABLE 7 Upregulated differentially expressed genes (DEGs) in TRAMP 5-month transgenic (TG) compared to wild type (WT) prostate macrophages

Gene	Accession #	Fold change	Normalized WT	counts TG
Arg1 <sup>b</sup>	NM_007482.3	At least 7.80	Below thresh- old	156.07
Fn1 <sup>b</sup>	NM_010233.1	6.82	48.96	334.07
Adam8 <sup>b</sup>	NM_007403.2	6.26	43.81	274.09
Chil3	NM_009892.2	At least 6.06	Below thresh- old	121.25
Cd38	NM_007646.4	5.94	38.66	229.59
Mmp19	NM_021412.2	5.33	24.91	132.86
Tuba1a	NM_011653.2	3.69	85.04	313.44
Ccl6 <sup>b</sup>	NM_009139.2	3.45	121.12	417.91
Ccl8 <sup>b</sup>	NM_021443.2	3.36	404.60	1358.87
Irf7 <sup>b</sup>	NM_016850.2	3.32	36.08	119.96
Ctsd <sup>a,b,c</sup>	NM_009983.2	3.31	2294.45	7601.78
Lag3	NM_008479.1	3.22	30.07	96.74
Chil4	NM_145126.2	At least 3.10	Below thresh- old	61.91
Ear3	NM_017388.1	At least 3.10	Below thresh- old	61.91
Amica1	NM_001005421.4	2.95	35.22	103.83
Fyn <sup>b</sup>	NM_008054.2	2.83	58.41	165.10
Fcgr2b <sup>a,b,c</sup>	NM_001077189.1	2.77	675.19	1867.72
Emp1 <sup>b</sup>	NM_010128.4	2.57	94.49	242.49
Cc19 <sup>b</sup>	NM_011338.2	2.54	897.68	2279.83
Cd84 <sup>a,b</sup>	NM_001252472.1	2.44	185.55	453.39
Tgm2 <sup>b</sup>	NM_009373.3	2.44	295.50	721.68
Hist1h1c	NM_015786.3	2.40	230.22	552.06
Тор2а	NM_011623.2	2.32	71.30	165.75
Fcgr4 <sup>b</sup>	NM_144559.1	2.29	181.25	414.69
C4a <sup>b</sup>	NM_011413.2	2.24	256.85	575.92
Vegfa <sup>a,b</sup>	NM_001025250.3	2.21	182.97	403.73
Apoe <sup>a,b,c</sup>	NM_001305844.1	2.16	10583.17	22829.21
Tlr8 <sup>b</sup>	NM_133212.2	2.12	201.87	427.59
Grn <sup>a,b,c</sup>	NM_008175.4	2.02	550.63	1110.57
Mertk	NM_008587.1	1.96	62.71	123.18
Vcam1	NM_011693.2	1.93	317.84	613.33
Ccr2 <sup>b</sup>	NM_009915.2	1.89	79.89	150.91

TABLE 7 (Continued)

	, ,			
C	A	Fold	Normalized	
Gene	Accession #	change	WT	TG
Anxa1 <sup>b</sup>	NM_010730.2	1.86	66.14	123.18
Ccr1 <sup>a,b</sup>	NM_009912.4	1.82	193.28	350.84
Fcgr1 <sup>b</sup>	NM_010186.5	1.81	354.78	641.70
Serpinb6a	NM_001164117.1	1.78	88.48	157.36
Itgam	NM_001082960.1	1.77	302.38	534.00
Txn1 <sup>a,b</sup>	NM_011660.3	1.70	621.93	1059.62
Adgre5	NM_011925.1	1.68	128.85	216.70
Mif <sup>b</sup>	NM_010798.2	1.68	158.06	265.71
Isg15 z <sup>a,b,c</sup>	NM_015783.3	1.65	181.25	298.60
Tlr13	NM_205820.1	1.64	217.33	355.36
Acly	NM_134037.2	1.61	154.62	248.94
Csf2rb <sup>b</sup>	NM_007780.4	1.57	284.34	446.29
S100a4	NM_011311.2	1.56	160.64	250.23
Trem2 <sup>b</sup>	NM_031254.2	1.53	305.81	466.93
Fcgr3	NM_010188.5	1.48	801.47	1187.96
Cd47 <sup>b</sup>	NM_010581.3	1.47	300.66	441.13
Hist2h2aa1	NM_013549.2	1.44	673.47	972.55
Ctnnb1 <sup>b</sup>	NM_007614.2	1.43	547.20	781.01
C1qb <sup>b</sup>	NM_009777.2	1.38	3853.58	5321.96

Abbreviation: TRAMP, transgenic adenocarcinoma of the mouse prostate. <sup>a</sup>Commonly upregulated across cohorts in TG compared to strainmatched, age-matched WT.

(Agilent). Gene expression was analyzed with nSolver software 4.0 (NanoString Technologies). The expression levels of each gene were normalized to those of control genes. Heat maps and unsupervised hierarchical clustering were generated in nSolver with agglomerative cluster analysis using average Euclidean distance. All genes with significant differential expression of p < .01 between strain-matched, age-matched TG and WT cohorts are listed in Tables 1-8. Thresholds for all genes were set to 20 counts.

#### 2.7 Statistical analysis

Differentially expressed gene analyses were performed in nSolver software 4.0 (NanoString Technologies) using the Differential Expression Call Error Model. Statistical analysis for IHC quantification analyses were performed using GraphPad Prism version 8. Outliers

<sup>&</sup>lt;sup>b</sup>Commonly upregulated across cohorts in Hi-Myc 6 months and TRAMP 5 months.

<sup>&</sup>lt;sup>c</sup>Commonly upregulated across cohorts in Hi-Myc 2 months, Hi-Myc 6 months, TRAMP 2 months, and TRAMP 5 months.

9

**TABLE 8** Downregulated differentially expressed genes (DEGs) in TRAMP 5-month transgenic (TG) compared to wild type (WT) prostate macrophages

Gene	Accession #	Fold change	Normalized WT	TG
Adamts1 <sup>b</sup>	NM_009621.4	-14.25	578.98	40.63
II12b <sup>b</sup>	NM_001303244.1	-12.78	4072.63	318.60
Mmp12 <sup>b</sup>	NM_008605.3	-9.39	4453.18	474.02
Mmp9 <sup>b</sup>	NM_013599.2	-6.50	427.79	65.78
Tnf <sup>b</sup>	NM_013693.2	-6.45	1822.85	282.48
Cxcl1	NM_008176.1	-5.96	6806.04	1142.17
Ccr7	NM_007719.2	-5.76	367.66	63.85
Plau <sup>b</sup>	NM_008873.2	-5.60	3150.90	562.38
Gem <sup>b</sup>	NM_010276.3	-4.86	548.92	112.86
Ccl22	NM_009137.2	-4.86	397.73	81.91
Ccl3, <sup>b</sup>	NM_011337.1	-4.72	16382.43	3471.65
Cyr61	NM_010516.1	At least -4.64	92.77	Below thresh- old
II1a	NM_010554.4	-4.54	626.23	138.01
Ripk2	NM_138952.3	-4.50	214.76	47.72
Areg	NM_009704.3	At least -4.34	86.76	Below thresh- old
Maff	NM_010755.3	-4.29	365.08	85.13
lfnb1	NM_010510.1	-4.19	624.51	148.98
Irf1 <sup>b</sup>	NM_008390.1	-4.17	940.63	225.73
H2-Eb1 <sup>b</sup>	NM_010382.2	-4.05	373.68	92.22
Icam1	NM_010493.2	-4.03	468.17	116.09
H2-Ea-ps <sup>b</sup>	NM_010381.2	-4.00	5752.02	1438.84
Malt1	NM_172833.2	-3.94	505.96	128.34
Cd40	NM_011611.2	-3.90	251.69	64.49
Icosl <sup>b</sup>	NM_015790.3	-3.75	1401.93	373.41
Nlrp3	NM_145827.3	-3.74	1260.19	336.65
Ccl4 <sup>b</sup>	NM_013652.1	-3.72	3965.25	1066.71
Cxcl2	NM_009140.2	-3.72	7675.37	2061.84
Tnfrsf12a	NM_001161746.1	-3.67	747.35	203.80
Hpgd <sup>b</sup>	NM_008278.2	-3.65	548.06	150.27
Hbegf	NM_010415.1	-3.62	133.15	36.76
Btg2 <sup>b</sup>	NM_007570.2	-3.41	1407.94	413.40
Nfkbiz <sup>b</sup>	NM_030612.1	-3.40	1962.01	576.57
Sqstm1 <sup>a</sup>	NM_011018.2	-3.39	3775.41	1113.79
Kitl	NM_013598.1	-3.38	141.74	41.92

TABLE 8 (Continued)

Gene	Accession #	Fold change	Normalized WT	TG
Tuba4a <sup>b</sup>	NM_009447.3	-3.36	164.93	49.01
Dusp2	NM_010090.2	-3.34	400.30	119.96
Traf1	NM_009421.3	-3.26	107.38	32.89
Skil	NM_011386.2	-3.25	2134.67	655.89
Cd83	NM_009856.2	-3.24	9731.88	3004.73
Cd69	NM_001033122.3	-3.23	137.44	42.57
Tnfaip3	NM_009397.2	-3.08	3514.26	1141.52
Jun <sup>b</sup>	NM_010591.2	-3.06	3102.79	1012.54
Nfkb1	NM_008689.2	-2.97	926.89	312.15
Cd86	NM_019388.3	-2.89	1693.99	586.24
Batf	NM_016767.2	-2.89	329.86	114.15
H2-Ob <sup>b</sup>	NM_010389.3	-2.80	232.80	83.20
Ptgs2	NM_011198.3	-2.79	3070.15	1098.96
II10	NM_010548.1	-2.77	155.48	56.11
Mmp13	NM_008607.1	-2.77	369.38	133.50
Cd36	NM_007643.3	-2.76	1201.77	435.33
II1b	NM_008361.3	-2.75	5181.63	1885.13
Tlr2	NM_011905.2	-2.73	2097.74	769.40
Sema4a	NM_013658.3	-2.73	207.88	76.10
Gadd45b	NM_008655.1	-2.70	1660.49	614.62
Rab20	NM_011227.1	-2.61	1502.43	574.63
Nfkbia	NM_010907.2	-2.55	974.13	382.44
Insig1 <sup>b</sup>	NM_153526.5	-2.53	485.35	191.54
Clic4	NM_013885.2	-2.47	552.35	223.79
ler3	NM_133662.2	-2.46	1203.49	488.86
Retnla	NM_020509.3	-2.45	2962.77	1209.89
Atf3 <sup>b</sup>	NM_007498.3	-2.45	6289.77	2570.04
Pdgfb	NM_011057.3	-2.41	321.27	133.50
Birc2	NM_007465.2	-2.38	249.98	105.12
Klf10 <sup>b</sup>	NM_013692.2	-2.36	217.33	92.22
Ccrl2	NM_017466.4	-2.34	6117.96	2619.70
Myc <sup>b</sup>	NM_010849.4	-2.30	240.53	104.48
Birc3	NM_007464.3	-2.29	632.24	276.67
Nr4a1 <sup>b</sup>	NM_010444.1	-2.29	864.18	377.28
Cxcl10	NM_021274.1	-2.26	1708.60	757.15
Map2k3	NM_008928.4	-2.26	284.34	125.76
Cxcl16	NM_023158.6	-2.24	5679.86	2538.44
C3	XM_011246258.1	-2.24	396.87	177.36

(Continues) (Continues)

TABLE 8 (Continued)

Gene	Accession #	Fold change	Normalized WT	d counts TG
Pdgfa	NM_008808.3	-2.21	396.01	179.29
Tlr9	NM_031178.2	-2.20	302.38	137.37
Rgs1	NM_015811.1	-2.19	3369.95	1539.45
Gsn <sup>a</sup>	NM_146120.3	-2.16	484.49	223.79
II1r2	NM_010555.4	-2.16	116.83	54.17
Hpgds	NM_019455.4	-2.13	538.61	252.81
Marcksl1 <sup>a,b</sup>	NM_010807.4	-2.13	761.95	357.94
Mob3c	NM_175308.4	-2.09	99.65	47.72
Hivep1	NM_007772.2	-2.07	224.21	108.35
F11r <sup>b</sup>	NM_172647.2	-2.06	248.26	120.60
Vasp <sup>a</sup>	NM_009499.2	-2.05	721.58	352.13
Nfkbie	NM_008690.3	-2.05	330.72	161.23
Col14a1 <sup>b</sup>	NM_181277.3	-2.04	646.84	317.31
Tlr1	NM_030682.1	-2.02	329.01	162.52
Cd14	NM_009841.3	-2.02	4630.14	2289.50
Peli1	NM_023324.2	-2.01	578.12	287.64
Ptafr	NM_001081211.1	-2.00	1607.23	802.29
ld2	NM_010496.3	-1.98	5803.56	2929.27
Vav1	NM_011691.4	-1.98	839.27	423.07
Н2-Аа	NM_010378.2	-1.96	49289.90	25211.58
Cd74	NM_001042605.1	-1.92	52908.97	27566.86
Cxcl3 <sup>a</sup>	NM_203320.2	-1.91	203.59	106.41
Gpr183	NM_183031.2	-1.90	325.57	170.91
lgf1r	NM_010513.2	-1.88	182.11	96.74
Ccl2	NM_011333.3	-1.87	3364.79	1800.64
II21r	NM_021887.1	-1.86	444.97	239.27
II10ra	NM_008348.2	-1.82	586.71	323.11
H2-Ab1	NM_207105.2	-1.81	13811.38	7618.55
AxI	NM_009465.3	-1.79	2632.05	1474.31
Socs3	NM_007707.2	-1.78	715.57	401.15
Rgl1	NM_016846.3	-1.77	174.38	98.67
Cxcl9	NM_008599.2	-1.76	163.21	92.87
Irf8	NM_008320.3	-1.76	323.85	184.45
Cd163 <sup>b</sup>	NM_053094.2	-1.75	346.19	197.99
Tgfbr1	NM_009370.2	-1.73	2756.61	1596.20
Ets1	NM_001038642.1	-1.72	175.24	101.90
II10rb	NM_008349.5	-1.72	1634.72	948.05
Stat6	NM_009284.2	-1.70	512.84	302.47

TABLE 8 (Continued)

Gene	Accession #	Fold change	Normalize WT	d counts TG
Traf2	NM_009422.2	-1.70	147.75	87.07
Fscn1 <sup>b</sup>	NM_007984.2	-1.70	144.32	85.13
lfnar1	NM_010508.1	-1.68	691.51	410.82
Arhgef6	NM_152801.2	-1.67	363.37	217.99
Clec5a	NM_001038604.1	-1.66	201.87	121.25
Il6ra	NM_010559.2	-1.65	256.85	156.07
Tgfbr2	NM_029575.3	-1.62	1986.92	1229.88
Irf5	NM_001252382.1	-1.60	700.10	437.91
Stat3	NM_213659.2	-1.60	477.62	297.96
II13ra1	NM_133990.4	-1.59	483.63	304.41
Cxcl13 <sup>b</sup>	NM_018866.2	-1.58	293.79	185.74
Cd180	NM_008533.2	-1.58	256.85	162.52
Ccl5	NM_013653.1	-1.58	299.80	190.25
Н2-DМа	NM_010386.3	-1.57	819.51	521.10
Fem1c	NM_173423.4	-1.56	595.30	381.80
Cybb	NM_007807.2	-1.56	1993.79	1281.47
Dusp1	NM_013642.3	-1.54	2810.72	1829.02
Klf4	NM_010637.3	-1.53	370.24	241.20
Smad7	NM_001042660.1	-1.53	222.49	145.75
Csf1r	NM_001037859.1	-1.52	3047.81	2007.67
Nampt	NM_021524.1	-1.51	666.60	440.49
Lat2	NM_020044.2	-1.51	329.01	217.99
H2-K1	NM_001001892.2	-1.48	6023.47	4082.40
Serpine1	NM_008871.2	-1.43	444.12	309.57
Vwa5a	NM_172767.3	-1.43	344.47	241.20
C3ar1	NM_009779.2	-1.43	2108.04	1474.95
II1rn	NM_031167.5	-1.42	856.45	604.30
Cxcl14	NM_019568.2	-1.40	383.12	272.81
Cdkn1a	NM_007669.4	-1.40	603.89	430.17
Adgre1	NM_010130.1	-1.38	1803.09	1307.27
Furin	NM_011046.2	-1.38	657.15	476.60

Abbreviation: TRAMP, transgenic adenocarcinoma of the mouse prostate. <sup>a</sup>Commonly downregulated across cohorts in TG compared to strain-matched, age-matched WT.

were identified by Grubbs' test with a false discovery rate (q) = 0.05. All results are expressed as means  $\pm$  *SD*. Data were analyzed using one- or two-way analysis of variance as specified. Differences were considered significant at p < .05. Figures denote statistical significance of p < .05 as \*, p < .01 as \*\*\*, p < .001 as \*\*\*, p < .001 as \*\*\*\*.

 $<sup>^{\</sup>mathrm{b}}\mathrm{Commonly}$  downregulated across cohorts in Hi-Myc 6 months and TRAMP 5-months.

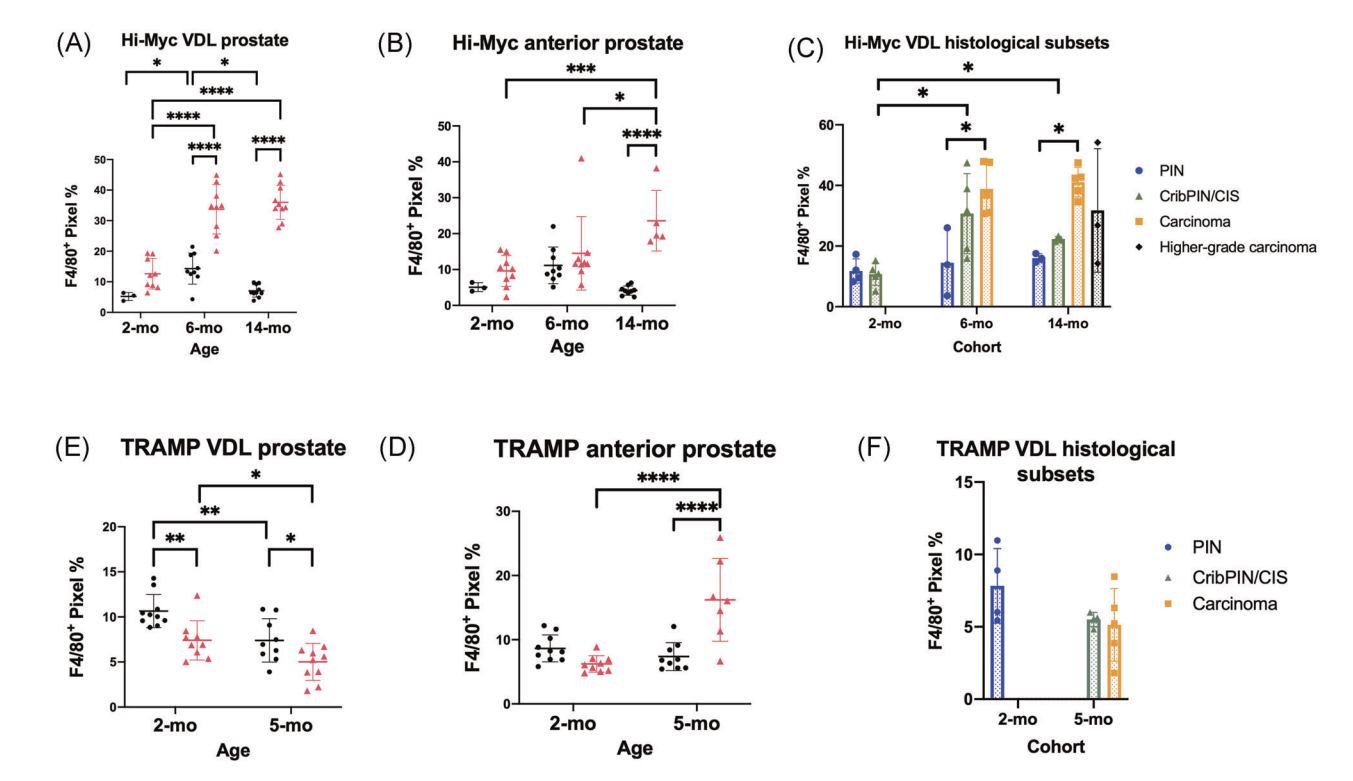


**FIGURE 1** Macrophage infiltration into Hi-Myc and TRAMP prostate tissue. Macrophage density was measured by quantification IHC staining of F4/80 $^{+}$  DAB stain pixels normalized to the sum of hematoxylin pixels and F4/80 $^{+}$  DAB stain pixels. Each data point represents one region in one mouse. Macrophage density was measured for different subsets: (A) Hi-Myc ventral and dorsolateral (VDL) lobes, (B) Hi-Myc anterior lobes, (D) TRAMP VDL lobes, and (E) anterior lobes. Regions of (C) Hi-Myc and (F) TRAMP prostate H&E tissue were classified histologically as prostatic intraepithelial neoplasia (PIN), cribriform PIN/carcinoma in situ (CribPIN/CIS), carcinoma, or higher-grade carcinoma. Significance was determined by two-way ANOVA with  $^*p < .05$ ,  $^{**}p < .01$ ,  $^{***}p < .001$ , and  $^{****}p < .0001$ . Black circles = WT. Pink triangles = TG. ANOVA, analysis of variance; H&E, hematoxylin and eosin; TG, transgenic; TRAMP, transgenic adenocarcinoma of the mouse prostate; WT, wild type [Color figure can be viewed at wileyonlinelibrary.com]

### 3 | RESULTS AND DISCUSSION

## 3.1 | Macrophage infiltration increases in Hi-Myc prostates with age, tumor presence, and histological grade

In an analysis of macrophage densities using IHC quantification of the pan-macrophage marker F4/80, Hi-Myc prostates exhibited an overall increase in macrophage density in TG prostates compared to WT prostates at each age group (2, 6, and 14 months) (Figure 1A). Increased macrophage density was also observed in Hi-Myc prostate tissue as it progressed in either age or histological grade (Figure 1A–C).

The changes in macrophage infiltration were mainly observed in the ventral and dorsolateral (VDL) lobes which are the sites of most precancer and invasive carcinoma development in Hi-Myc TG mice. Interestingly, however, increased macrophage density with presence of TG compared to WT and with increasing age was also observed in the adjacent anterior lobe tissue at 14 months (Figure 1B). While 10% of anterior lobes from 6 months old and 80% of anterior lobes from 14-month-old Hi-Myc mice contained regions of cribriform PIN/carcinoma in situ (CribPIN/CIS) or invasive adenocarcinoma.

The increase in macrophage infiltration in Hi-Myc TG VDL lobes was corroborated by flow cytometry analysis of macrophage populations. Macrophage levels were significantly increased in prostates from 6- and 14-month old Hi-Myc TG mice compared to all other cohorts (Figure 2A). Overall, these data suggest that in Hi-Myc mice development of adenocarcinoma tissue induces higher levels of macrophages in the prostate and is similar to the increases in macrophage density observed in prostate cancer patients.<sup>2</sup>

## 3.2 | Macrophage density by 3D spatial analysis varies widely throughout Hi-Myc prostate tumor tissue

To better understand macrophage spatial density throughout the tissue, 3D cell density analysis was performed on a representative 14-month Hi-Myc TG prostate. Macrophage densities varied across different regions of the tissue (Figure 3A–C). Total cell densities within a tumor (ROI1) were higher than tissue adjacent to tumor (ROI2). Macrophage densities proximal to ROI1 were lower than those proximal to ROI2 (Figure 3D,E). In this comparison, macrophage infiltration was higher in the tumor-adjacent tissue than in the

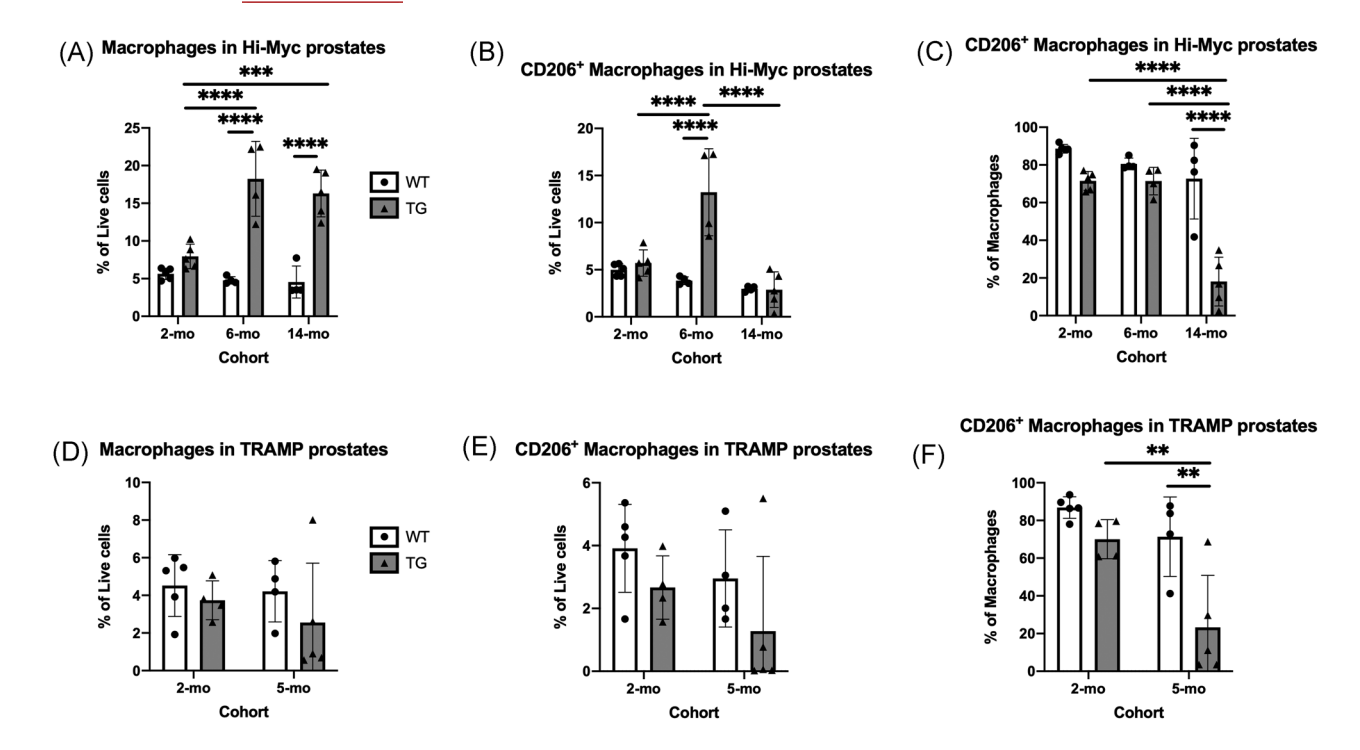


**FIGURE 2** Macrophage populations in Hi-Myc and TRAMP prostate tissue.  $CD45^{+}CD11b^{+}F4/80^{+}CD68^{+}$  macrophage populations were determined by flow cytometry. (A) Macrophages as a percentage of live cells in Hi-Myc prostates. (B)  $CD206^{+}$  macrophages as a percentage of live cells in Hi-Myc prostates. (C)  $CD206^{+}$  macrophages as a percentage of all macrophages in Hi-Myc prostates. (D) Macrophages as a percentage of live cells in TRAMP prostates. (E)  $CD206^{+}$  macrophages as a percentage of live cells in TRAMP prostates. (F)  $CD206^{+}$  macrophages as a percentage of all macrophages in TRAMP prostates. Significance was determined by two-way ANOVA with \*\*p < .01, \*\*\*p < .001, and \*\*\*\*p < .0001. WT = wild type (white bars, circles); TG = transgenic (grey bars, triangles); mo = month. ANOVA, analysis of variance; TRAMP, transgenic adenocarcinoma of the mouse prostate

middle of a large region of tumor tissue. This is generally the trend throughout other points within this prostate however there are regions of tumor tissue that have higher macrophage infiltration. The variation in macrophage density throughout the dimensions of the tissue speak to the complexity of macrophage biology and the importance of spatial heterogeneity when considering how macrophages function within tumors. The 3D analysis technique provides a useful tool and further opportunity for investigating where TAMs and other cell types are acting within tumors. This information could be pertinent to determining how to target TAMs or other TME components.

## 3.3 | CD206<sup>+</sup> macrophage populations decrease in late-stage Hi-Myc tumors

The pro-tumor macrophage marker mannose receptor CD206 expression was analyzed by flow cytometry to begin to differentiate the broad phenotypic characteristics of macrophages in the different models. CD206<sup>+</sup> macrophage populations increased proportional to all live cells in 6-month-old TG mice compared to all other cohorts (Figure 2B). However, when analyzed as a proportion of macrophages, the percentage of CD206<sup>+</sup> macrophages did not change between cohorts except in 14-month-old TG mice in which CD206<sup>+</sup>

macrophage proportions decreased (Figure 2C). This suggests that as prostate macrophage populations increase with tumor growth from 2 to 6 months, the proportion of macrophages that are CD206<sup>+</sup> remains around 70%. As the tumor continues to grow out to 14 months, the number of CD206<sup>-</sup> macrophages overtake the number of CD206<sup>+</sup> macrophages. Because CD206 is a pro-tumor macrophage marker, it can be concluded that 60%–80% of macrophages in WT prostates and 2- to 6-month-old TG prostates have some pro-tumor characteristics. While only about 20% of 14-month-old prostate macrophages express the pro-tumor marker CD206, the pro- and anti-tumor characteristics of these macrophages was then further explored.

### 3.4 | Macrophages in Hi-Myc TG prostates exhibit increased pro-tumor gene expression profiles

To further delineate macrophage phenotype in the Hi-Myc mice, FACS-separated CD11b<sup>+</sup>F4/80<sup>+</sup> Hi-Myc prostate macrophages were analyzed for their myeloid gene expression by NanoString messenger RNA profiling. Overall, gene expression patterns of prostate macrophages from younger (2 months old) mice more closely resembled one another regardless of genotype, while older (6 and 14 months old) TG mice more closely resemble one another regardless of age

# cells in xy location

2

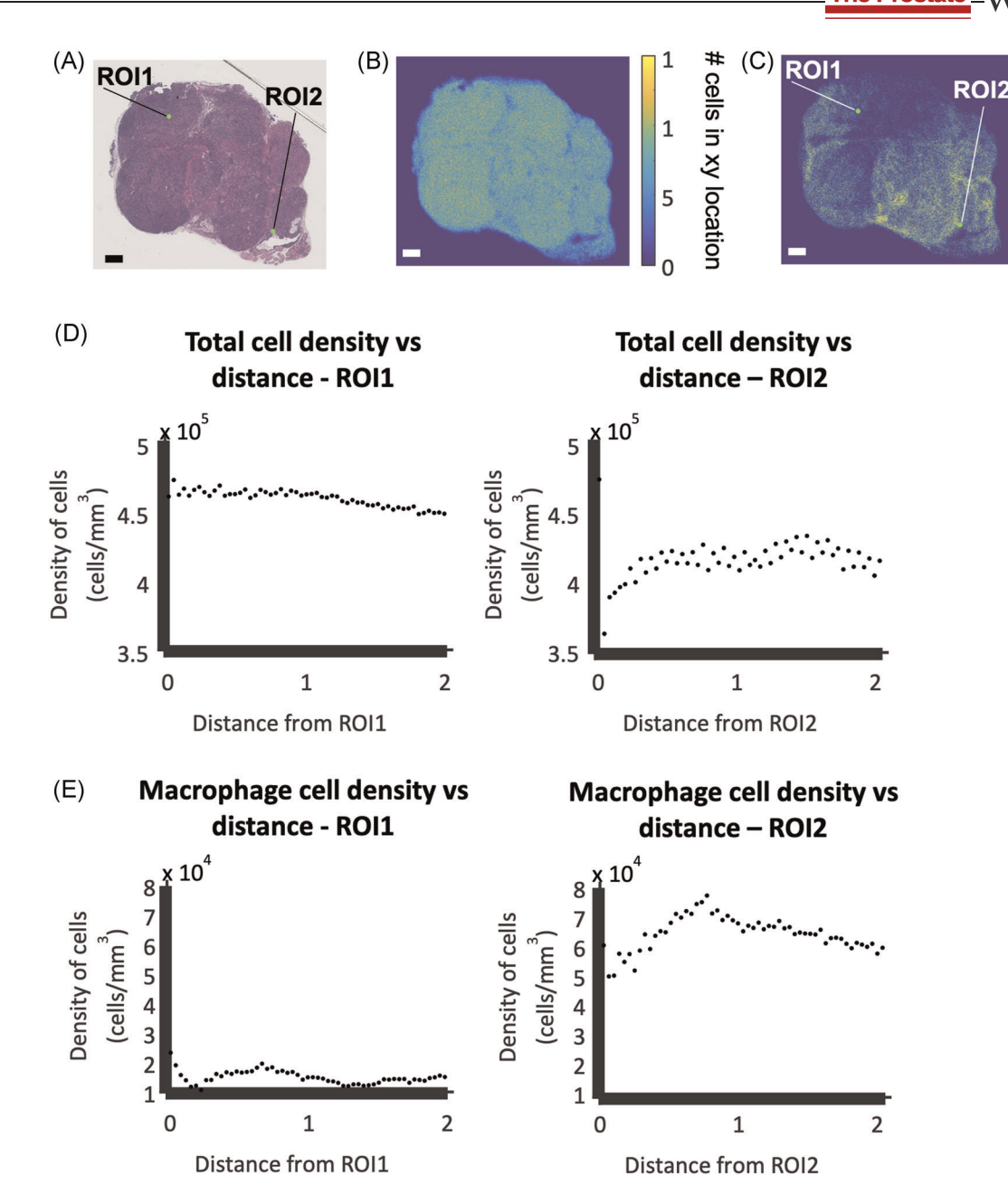


FIGURE 3 Macrophage 3D spatial analysis of Hi-Myc late-stage tumor. (A) H&E stain of a representative 4- $\mu$ m section of a representative Hi-Myc 14-month-old TG prostate with regions of interest ROI1 and ROI2. (B) Compressed Z projection of all cells in the representative section. (C) Compressed Z projection of F4/80<sup>+</sup> macrophages with ROI1 and ROI2. (D) Density of total cells measured by 3D density analysis compared to distance from ROI1 and ROI2. (E) Density of F4/80<sup>+</sup> macrophages measured 3D density analysis compared to distance from ROI1 and ROI2. Scale bar = 2 mm. 3D, three dimensional; H&E, hematoxylin and eosin [Color figure can be viewed at wileyonlinelibrary.com]

(Figure 4A). The Hi-Myc 14-month WT sample was omitted as the sample input was below threshold. When limiting the analysis to key pro-tumor and anti-tumor macrophage genes, a similar trend was observed with the exception of 6-month WT macrophages clustering with 2-month WT and TG macrophages (Figure 4B). This suggests that tumor presence and growth is more influential on macrophage characteristics than age. Overall, prostate macrophages from Hi-Myc TG mice exhibited higher pro-tumor (Cd206, Arg1, II10, Vegfa, and Pdl1) and lower antitumor (Tnf, II1b, II12b, Cd80, and Cd86) macrophage gene expression compared to age-matched WT mice (Figure 4C-F). While not all genes (i.e., II1b and Cd80) followed this

pattern, taken cumulatively the tumor-infiltrating prostate macrophages exhibited more pro-tumor characteristics which was further supported by the expression of various inflammatory genes including Adam8, Adamst1, Ccl3, Cxcl13, Il1rn, Mmp9, and Mmp12 (Tables 1–4).

Notably, detection of CD206 differed between NanoString RNA expression analysis and flow cytometry surface protein expression. This is likely due to differences in RNA and protein expression and detection with flow cytometry detection of surface protein likely being the more biologically relevant assessment of CD206 expression. Apart from this discrepancy, prostate macrophages tended to demonstrate an overall pro-tumor RNA

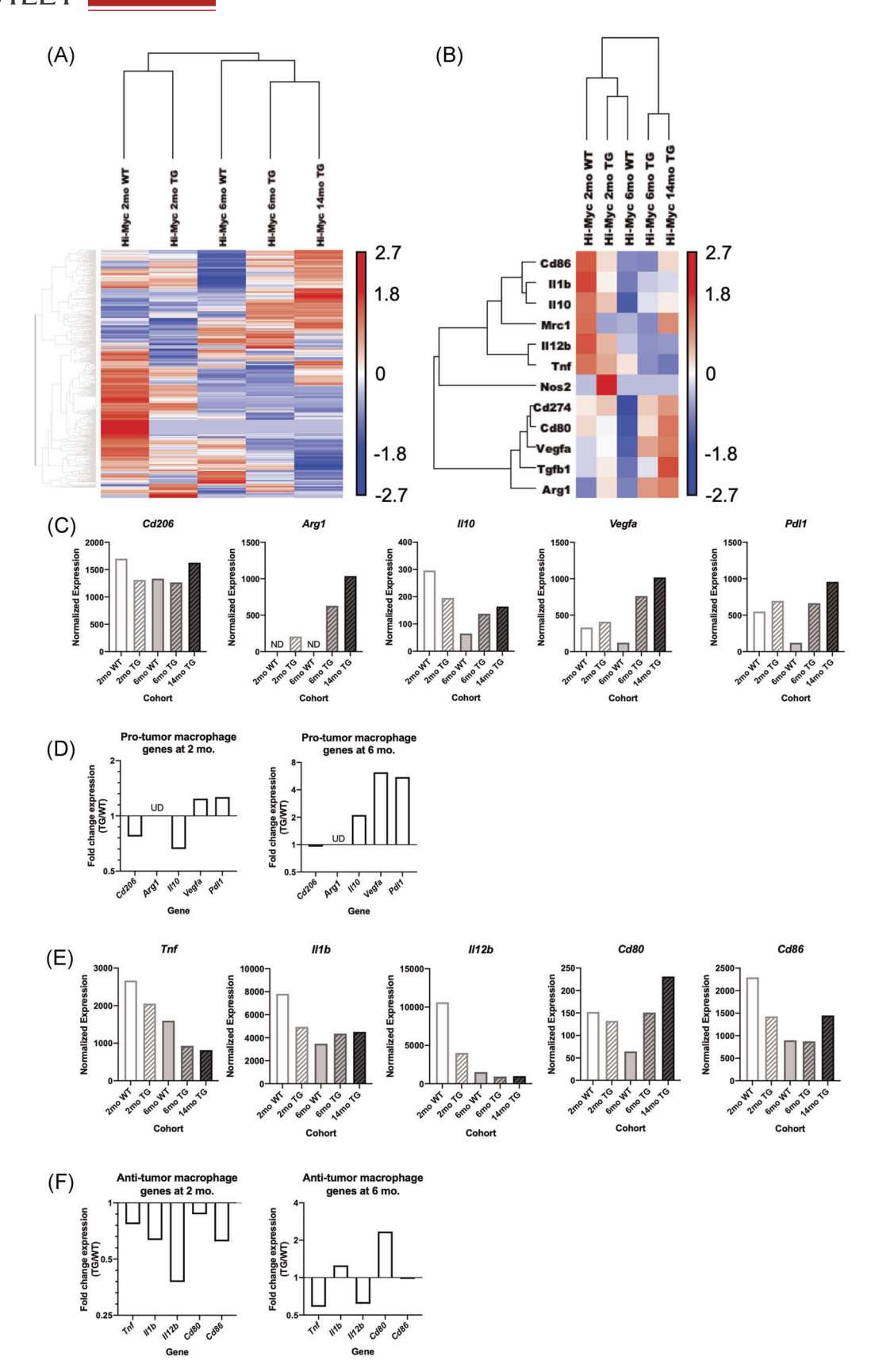


FIGURE 4 (See caption on next page)

expression and decrease in overall antitumor RNA expression in tumor-bearing mice.

Taken together, these data suggest that Hi-Myc adenocarcinoma tumor growth increases both macrophage density and the pro-tumor characteristics of infiltrating macrophages.

### 3.5 | Macrophage infiltration decreases in TRAMP prostates with tumor presence and age

When similar analyses were applied to TRAMP tissue, an opposite pattern of macrophage infiltration from the Hi-Myc mice was observed with decreased macrophage density in TRAMP TG tissue compared to WT at both 2 and 5 months (Figure 1D). Additionally, when comparing different ages within the same genotype, macrophage density decreased with age. However, no significant difference in macrophage density was observed between different histological lesion types within TRAMP TG VDL tissue (Figure 1F).

Counter to TRAMP VDL tissue but similar to Hi-Myc anterior tissue, macrophage density increased in older (5 months old) TRAMP TG anterior prostates (Figure 1E). At this age, 14% of anterior lobe samples had invasive carcinoma or CribPIN/CIS regions. However, given that disease stage did not correlate with higher macrophage density in TRAMP TG VDL, this increase in TG anterior lobe tissue is likely due to other factors such as increased stress and inflammation in the surrounding tumoradiacent tissue.

Similar to the IHC results, flow cytometry analysis of macrophage populations in VDL tissue revealed that macrophage levels decreased in prostates from 5-month-old TG mice compared to all other cohorts (Figure 2D). Altogether, these data suggest that macrophage populations decrease with TRAMP tumor growth.

## 3.6 | CD206<sup>+</sup> macrophage populations decrease in late-stage TRAMP tumors

Flow cytometry analysis showed a decrease in CD206<sup>+</sup> macrophage populations in TRAMP TG mice compared to WT with the largest decrease at 5 months (Figure 2E). Additionally, the same trend was

observed when analyzing CD206<sup>+</sup> macrophages as a proportion of all macrophages (Figure 2F). Similar to Hi-Myc mice, 60%–80% of macrophages in WT prostates and 2-month-old TRAMP TG prostates express the pro-tumor marker CD206. Also similar to Hi-Myc mice, only about 20% of macrophages from late stage tumor bearing mice express CD206. This suggests that as tumors grow and macrophage populations decrease, the proportion of macrophages that express CD206 also decrease. The following subsection further explores the pro- and antitumor characteristics of these macrophages with a larger array of genes.

# 3.7 | Macrophages in TRAMP TG prostates exhibit increased pro- and antitumor gene expression profiles at tumor initiation but decreased antitumor gene expression in late-stage tumors

FACS-separated macrophages from TRAMP prostates reveal that 5-month TG prostate macrophages have different expression profiles compared to 2-month WT, 2-month TG, and 5-month WT that all exhibit similar myeloid gene expression trends (Figure 5A). When limiting the analysis to key pro-and antitumor macrophage genes, a similar trend was observed with 2-month WT and TG macrophages closest in gene expression and 5-month WT macrophages more closely resembling 2-month WT and TG than 5-month TG macrophages (Figure 5B). Interestingly, the expression profiles of macrophages from 2-month TG and 5-month TG displayed opposite expression profiles suggesting macrophage expression changes drastically from early- to late-stage tumors (Figure 5C-F). This pattern of expression is also observed when limited to pro-tumor (Cd206, Arg1, II10, Vegfa, and PdI1) and antitumor (Nos2, Tnf, II1b, II12b, Cd80, and Cd86) macrophage gene expression with 2-month TG macrophages expressing high levels of all pro- and antitumorassociated genes but low levels of Arg1 while 5-month TG macrophages expressed low levels of most pro- and antitumor-associated genes but high levels of Arg1. Unlike with Hi-Myc prostates, the decrease in CD206 expression in TRAMP prostates was consistent between RNA NanoString and flow cytometry analyses. Looking at select representative pro- and antitumorigenic macrophage RNA transcripts, prostate macrophages from 2-month-old TRAMP TG mice exhibit increase expression of both subsets suggesting these macrophages are generally more inflammatory compared to agematched WT prostate macrophages. The reason for this is unknown,

FIGURE 4 Hi-Myc transgenic prostate macrophages express higher levels of pro-tumor genes. Hi-Myc wild type (WT) and transgenic (TG) prostate macrophages from 2-, 6-, and 14-month-old mice were analyzed by NanoString Myeloid Panel gene expression analysis. (A) Dendrograms and heat map of gene expression across all Myeloid Panel genes that were detected above background in at least one sample compared between each cohort. (B) Dendrograms and heat map of gene expression across select pro- and antitumor macrophage genes that were detected above background in at least one sample compared between each cohort. (C) Select pro-tumor macrophage genes normalized to control genes. (D) Fold change expression of pro-tumor macrophage genes in age-matched TG tissue relative to WT. (E) Select antitumor macrophage genes normalized to control genes. (F) Fold change expression of antitumor macrophage genes in age-matched TG tissue relative to WT. Heat maps were generated using unsupervised hierarchical clustering with average Euclidean distance. ND = not detected; UD = undefined due to below threshold expression of WT control [Color figure can be viewed at wileyonlinelibrary.com]

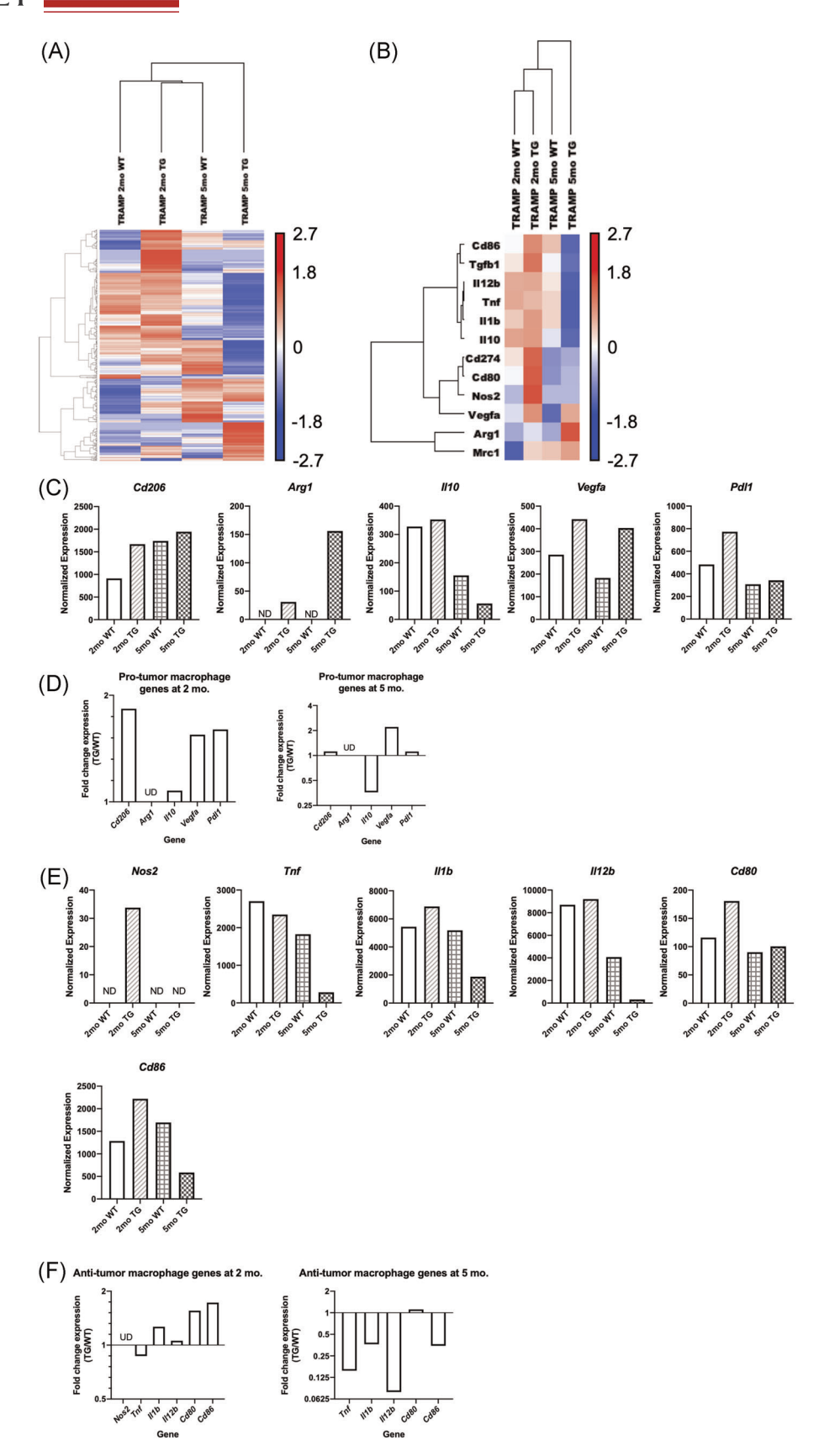


FIGURE 5 (See caption on next page)

though it is likely a response to the initial stages of tumor development and tissue reconstruction observed at this age in TRAMP mice. Hive-month-old TRAMP TG prostate macrophages exhibited more protumorigenic characteristics than those in the age-matched WT tissue, expressing higher levels of some protumorigenic genes and decreased levels of many antitumorigenic genes. As with the Hi-Myc mice, not all genes followed this pattern, but the cumulative gene expression changes point towards a more pro-tumor macrophage characteristic which was corroborated by various inflammatory genes such as *Ccr1*, *Cd84*, and *Cxcl3* in the Differential Expression Call analyses (Tables 5–8). Altogether these data suggest that while TRAMP neuroendocrine tumor growth decreases macrophage density, it increases the pro-tumor characteristics of infiltrating macrophages.

## 3.8 | Hi-Myc and TRAMP TAMs share common differentially regulated genes

Though Hi-Myc and TRAMP models exhibited unique macrophage characteristics, some similarities were also observed. Increases in Apoe (apolipoprotein E), Ctsd (cathepsin D), Fcgr2b (Fc receptor, immunoglobulin G, low affinity IIb), Grn (granulin), and Isg15 (interferon-stimulated gene 15 ubiquitin-like modifier) were observed in all TG cohorts compared to age-matched WT mice. Apoe is a low-density lipoprotein ligand and promotes cholesterol uptake.<sup>25</sup> Ctsd promotes lysosomal activity and autophagy.<sup>25</sup> Fcgr2b is involved in antibody-mediated phagocytosis.<sup>26</sup> Grn promotes inflammation, is associated with proliferation, and promotes lysosomal function. 27,28 Isg15 has a variety of functions that include resolving viral infections, promoting exosome secretion, promoting cholesterol efflux, and promoting several inflammatory responses.<sup>29,30</sup> Altogether these upregulated genes may play various roles in lipid metabolism, lysosomal activity, and the general inflammatory response of TAMs in these models. Targeting these proteins or their related pathways may provide a powerful method for disrupting TAM tumor promotion.

Interestingly, *Ccr2* expression is upregulated in TG prostates compared to WT in both Hi-Myc and TRAMP models. While Further investigation is needed to fully understand the origin of these TAMs,

this suggests that macrophages in these tumors may be infiltrating from the circulation rather than arising from local proliferation.

It should be noted that in both 6-month-old Hi-Myc and 5-month-old TRAMP TG mice *Cd163* expression unexpectedly decreased compared to age-matched WT mice. *Cd163* is often used as a pro-tumor macrophage marker, but in these instances was found to be decreased in pro-tumor macrophages from late-stage tumors. Thus, *Cd163* is not an effective marker for assessing pro- or antitumor characteristics of TAMs in Hi-Myc and TRAMP models.

### 3.9 | Hi-Myc is a more representative model than TRAMP for prostate cancer TAM studies

These macrophage studies reveal that the two prostate cancer TG models exhibit key similarities and differences in their TME. While macrophage infiltration increased with age and histological grade in Hi-Myc mice, the opposite was observed in TRAMP mice. However, the two models exhibited similar trends of increased pro-tumor gene expression in prostate macrophages with increasing age and presence of tumor in TG mice. This is consistent with current knowledge of TAM pro-tumor functions. The differences in TAM infiltration may be due to the differences in cancer type and biology as Hi-Myc tumors are more adenocarcinoma-like and TRAMP tumors neuroendocrine-like. Since adenocarcinoma is more commonly seen in patients, the Hi-Myc model is likely more representative of TAMs present in most patient tumors.<sup>2</sup> The difference in macrophage density trends between the two models suggests that TAMs play different roles in supporting these two cancer types. The increase in macrophage density in tumors from patients and Hi-Myc TG mice may suggest that macrophagetargeted therapies would be more effective against prostate adenocarcinomas. Due to its similarity to patient TAM trends, the Hi-Myc model is a better model for prostate cancer TAM-related studies. Ongoing work uses the Hi-Myc model to investigate prostate cancer TAM biology and macrophage-targeted therapeutic approaches. With this novel information on TAM characteristic in this model, prostate cancer research is better equipped to advance TAM-focused therapies.

FIGURE 5 TRAMP transgenic prostate macrophages express higher levels of pro-tumor genes. TRAMP wild type (WT) and transgenic (TG) prostate macrophages from 2- and 5-month-old mice were analyzed by NanoString Myeloid Panel gene expression analysis. (A) Dendrograms and heat map of gene expression across all Myeloid Panel genes that were detected above threshold (20 counts) in at least one sample compared between each cohort. (B) Dendrograms and heat map of gene expression across select pro- and antitumor macrophage genes that were detected above threshold (20 counts) in at least one sample compared between each cohort. (C) Select pro-tumor macrophage genes normalized to control genes. (D) Expression of pro-tumor macrophage genes in age-matched TG tissue relative to WT. (E) Select antitumor macrophage genes normalized to control genes. (F) Expression of antitumor macrophage genes in age-matched TG tissue relative to WT. Heat maps were generated using unsupervised hierarchical clustering with average Euclidean distance. ND = not detected; UD = undefined due to below threshold expression of WT control. TRAMP, transgenic adenocarcinoma of the mouse prostate [Color figure can be viewed at wileyonlinelibrary.com]

### 4 | CONCLUSION

Prostate cancer treatments currently neglect the role of the TME and TAMs in supporting cancer. Many in vivo models used for studying cancer do not properly recapitulate the complex TME. Studying TAMs in TG prostate cancer models which reflect more accurate TMEs may lead to more impactful studies for TAM-targeted therapies. TAMs from Hi-Myc adenocarcinoma and TRAMP neuroendocrine TG models on the FVB/N background both exhibit protumor characteristics. However, there are key differences in macrophage infiltration levels with Hi-Myc tumors containing higher and TRAMP tumors containing lower macrophage densities than agematched WT prostates. Because patient tumors are more often adenocarcinomas and also exhibit higher macrophage densities than normal prostate tissue, the Hi-Myc model should function as a more representative model for investigating prostate cancer TAM biology and pursuing TAM-targeted therapies.

### **ACKNOWLEDGEMENTS**

The authors thank the members of the Johns Hopkins Urology Department, the Johns Hopkins Oncology Department, and the Pienta Lab, especially Kenneth C. Valkenburg, for training and thoughtful discussion. This work was supported by US Department of Defense CDMRP/PCRP (W81XWH-17-1-0528) for W.N. Brennen; NCI SPORE grant in Prostate Cancer P50CA58236 and the NCI U01CA196390 for the Molecular and Cellular Characterization of Screen Detected Lesions (MCL) for A.M. De Marzo; US Department of Defense CDMRP/PCRP (W81XWH-20-1-0353), the Patrick C. Walsh Prostate Cancer Research Fund, and the Prostate Cancer Foundation to S.R. Amend: NCI grants U54CA143803, CA163124. CA093900, and CA143055, and the Prostate Cancer Foundation to K.J. Pienta. This work was also supported by the William and Carolyn Stutt Research Fund, Ronald Rose, MC Dean, Inc., William and Marjorie Springer, Mary and Dave Stevens, Louis Dorfman, the Jones Family Foundation, Timothy Hanson, and the David and June Trone Family Foundation.

### **CONFLICT OF INTERESTS**

Denis Wirtz is a cofounder and owns stock in AbMeta Therapeutics, Inc. Angelo M. De Marzo receives research support from Janssen R&D and Myriad and is a consultant for Cepheid. Kenneth J. Pienta is a consultant for CUE Biopharma, Inc., is a founder and holds equity interest in Keystone Biopharma, Inc., and receives research support from Progenics, Inc.

### DATA AVAILABILITY STATEMENT

The data that support the findings of this study are available from the corresponding author upon reasonable request.

### ORCID

Amber E. de Groot https://orcid.org/0000-0002-4506-1910

Kayla V. Myers http://orcid.org/0000-0002-0748-1092

Timothy E. G. Krueger http://orcid.org/0000-0002-7477-4012

W. Nathaniel Brennen https://orcid.org/0000-0001-9807-7433

Sarah R. Amend https://orcid.org/0000-0002-5606-1262

Kenneth J. Pienta https://orcid.org/0000-0002-4138-2186

### **REFERENCES**

- Roca H, Varsos ZS, Sud S, Craig MJ, Ying C, Pienta KJ. CCL2 and interleukin-6 promote survival of human CD11b+ peripheral blood mononuclear cells and induce M2-type macrophage polarization. *J Biol Chem.* 2009:284(49):34342-34354.
- Zarif JC, Baena-Del Valle JA, Hicks JL, et al. Mannose receptorpositive macrophage infiltration correlates with prostate cancer onset and metastatic castration-resistant disease. Eur Urol Oncol. 2019;2(4):429-436.
- 3. Craig M, Ying C, Loberg RD. Co-inoculation of prostate cancer cells with U937 enhances tumor growth and angiogenesis in vivo. *J Cell Biochem.* 2008;103(1):1-8.
- Aras S, Zaidi MR. TAMeless traitors: macrophages in cancer progression and metastasis. Br J Cancer. 2017;117(11):1583-1591.
- Rőszer T. Understanding the mysterious M2 macrophage through activation markers and effector mechanisms. *Mediators Inflamm*. 2015;2015:816460.
- Myers KV, Amend SR, Pienta KJ. Targeting Tyro3, Axl and MerTK (TAM receptors): implications for macrophages in the tumor microenvironment. Mol Cancer. 2019;18(1):94.
- Dalen FJ, van Stevendaal MHME, Fennemann FL, Verdoes M, Ilina O. Molecular repolarisation of tumour-associated macrophages. *Molecules*. 2018:24(1):9.
- Parayath NN, Parikh A, Amiji MM. Repolarization of Tumorassociated macrophages in a genetically engineered nonsmall cell lung cancer model by intraperitoneal administration of hyaluronic acid-based nanoparticles encapsulating microRNA-125b. *Nano Lett.* 2018;18(6):3571-3579.
- Rong L, Zhang Y, Li W-S, Su Z, Fadhil JI, Zhang C. Iron chelated melanin-like nanoparticles for tumor-associated macrophage repolarization and cancer therapy. *Biomaterials*. 2019;225:119515.
- Liao Z-X, Fa Y-C, Kempson IM, Tseng SJ. Repolarization of M2 to M1 macrophages triggered by lactate oxidase released from methylcellulose hydrogel. *Bioconjug Chem.* 2019;30(10):2697-2702.
- Yuan A, Hsiao Y-J, Chen H-Y, et al. Opposite effects of M1 and M2 macrophage subtypes on lung cancer progression. Sci Rep. 2015; 5(1):14273.
- Jayasingam SD, Citartan M, Thang TH, Mat Zin AA, Ang KC, Ch'ng ES. Evaluating the polarization of tumor-associated macrophages into M1 and M2 phenotypes in human cancer tissue: technicalities and challenges in routine clinical practice. Front Oncol. 2020;9:1512.
- Bercovici N, Guérin MV, Trautmann A, Donnadieu E. The remarkable plasticity of macrophages: a chance to fight cancer. Front Immunol. 2019;10(1563):1563.
- Becher OJ, Holland EC. Genetically engineered models have advantages over xenografts for preclinical studies. *Cancer Res.* 2006; 66(7):3355-3359.
- Olson B, Li Y, Lin Y, Liu ET, Patnaik A. Mouse models for cancer immunotherapy research. *Cancer Discovery*. 2018;8(11):1358-1365.
- Ellwood-Yen K, Graeber TG, Wongvipat J, et al. Myc-driven murine prostate cancer shares molecular features with human prostate tumors. *Cancer Cell*. 2003;4(3):223-238.
- Greenberg NM, DeMayo F, Finegold MJ, et al. Prostate cancer in a transgenic mouse. Proc Natl Acad Sci USA. 1995;92(8): 3439-3443.
- Chiaverotti T, Couto SS, Donjacour A, et al. Dissociation of epithelial and neuroendocrine carcinoma lineages in the transgenic adenocarcinoma of mouse prostate model of prostate cancer. Am J Pathol. 2008;172(1):236-246.

- Huss WJ, Maddison LA, Greenberg NM. Autochthonous mouse models for prostate cancer: past, present and future. Semin Cancer Biol. 2001;11(3):245-259.
- Watson PA, Ellwood-Yen K, King JC, Wongvipat J, Lebeau MM, Sawyers CL. Context-dependent hormone-refractory progression revealed through characterization of a novel murine prostate cancer cell line. Cancer Res. 2005;65(24):11565-11571.
- Kwon ED, Hurwitz AA, Foster BA, et al. Manipulation of T cell costimulatory and inhibitory signals for immunotherapy of prostate cancer. *Proc Natl Acad Sci USA*. 1997;94(15):8099-8103.
- Valkenburg KC, Amend SR, Pienta KJ. Murine prostate microdissection and surgical castration. JoVE. 2016;111:e53984.
- Iwata T, Schultz D, Hicks J, et al. MYC overexpression induces prostatic intraepithelial neoplasia and loss of Nkx3.1 in mouse luminal epithelial cells. PLoS One. 2010;5(2):e9427.
- Qian B-Z, Pollard JW. Macrophage diversity enhances tumor progression and metastasis. Cell. 2010;141(1):39-51.
- Getz GS, Reardon CA. Apoprotein E and reverse cholesterol transport. Int J Mol Sci. 2018;19(11):3479.
- Smith KGC, Clatworthy MR. Erratum: FcγRIIB in autoimmunity and infection: evolutionary and therapeutic implications. Nat Rev Immunol. 2010;10(9):674.
- 27. Eriksen JL, Mackenzie IR. Progranulin: normal function and role in neurodegeneration. *J Neurochem.* 2008;104(2):287-297.

- Götzl JK, Lang CM, Haass C, Capell A. Impaired protein degradation in FTLD and related disorders. Ageing Res Rev. 2016;32:122-139.
- Perng YC, Lenschow DJ. ISG15 in antiviral immunity and beyond. Nat Rev Microbiol. 2018;16(7):423-439.
- Huang C, Yu XH, Zheng XL, Ou X, Tang CK. Interferonstimulated gene 15 promotes cholesterol efflux by activating autophagy via the miR-17-5p/Beclin-1 pathway in THP-1 macrophage-derived foam cells. Eur J Pharmacol. 2018;827: 13-21.

#### SUPPORTING INFORMATION

Additional Supporting Information may be found online in the supporting information tab for this article.

How to cite this article: Groot AE, Myers KV, Krueger TEG, et al. Characterization of tumor-associated macrophages in prostate cancer transgenic mouse models. *The Prostate*. 2021; 1–19. https://doi.org/10.1002/pros.24139